Dynamical decoupling schemes for inhibiting decoherence in the propagation of single-photon polarization qubits

D. Vitali, G. Di Giuseppe, D. Sajeev, R. Kumar, M. Lucamarini, G. Ventura, P. Tombesi

Abstract— One of the fundamental limitations to high bit rate, long distance, telecommunication in optical fibers is Polarization Mode Dispersion (PMD). Here we show how one can adapt bang-bang control techniques for suppressing the decoherence of polarization states in optical fibers by carrying out controlled rotations of polarization at predetermined locations along the fiber. We propose an experimental proof-of-principle demonstration of the idea based on the propagation of polarization qubits in a ring-cavity containing birefringent crystals and wave-plates.

I. INTRODUCTION

Dynamical decoupling offers a versatile control toolbox for quantum dynamical engineering in both high-resolution spectroscopy [1] and quantum information science [2]. Decoupling schemes operate by subjecting the target system to a series of open-loop control transformations, in such a way that the net evolution is coherently modified to a desired one [3]. This avoids auxiliary memory and measurement resources, while additionally enabling straightforward integration with other passive [4] or active [5] quantum control techniques. Applications of decoupling range from the removal of undesired couplings in interacting quantum subsystems to active decoherence control and symmetrization in open quantum systems [6], [7].

Up to now almost all the experimental demonstration of decoupling techniques have been carried out within nuclear magnetic resonance (NMR) systems (see e.g. [7]). However propagation of photonic qubits along optical fibers could represent an important field of application of dynamical decoupling schemes for preventing decoherence. In such a case "bang-bang" techniques [7] have to be implemented "in space", rather than in time, i.e., along the fiber length [8]. In fact, polarization effects in single-mode fibers are a common source of problems both in classical optical communication schemes and in quantum ones [9]. Birefringence is the presence of two different phase velocities for two orthogonal polarization states. It is caused by asymmetries in the fiber geometry and in the residual stress distribution inside and around the core.

Polarization Mode Dispersion (PMD) arises because the residual birefringence changes randomly along the fiber, that is, both the orientation of its fast and slow axes and the

value of the difference between the two indexes of refraction randomly vary along the fiber. This results in random mode coupling as the light propagates. Because of this statistical process, the effects of PMD such as pulse spreading increase as the square root of the propagation distance [10], [11], [12], [13], [14]. This statistical process makes it extremely difficult to correct the effects of PMD after the light has propagated through a long length of fiber. PMD is a fundamental limitation on high speed, high bit rate communication in fiber systems because it distorts the shape of light pulses, and in particular induces pulse spreading. Hence much effort has gone into reducing PMD in optical fibers, see [15], [16] for reviews.

Two main methods have been devised to reduce PMD in optical fibers. The first is to minimize asymmetries in the index profile and stress profile of the fiber. To this end the manufacturing process has been steadily improved. The second method is to spin the fiber during the manufacturing process as described in [17], [18]. Our basic idea is different and amounts to introduce controlled polarization rotations at predetermined locations along the fiber in such a way that the effects of PMD are reduced [19]. As in bang-bang schemes, after several such controlled polarization rotations, the state of polarization of the light has been oriented along many different directions on the Bloch sphere in such a way that the effects of the fiber birefringence averages out. We expect that once that the main decoherence sources affecting a single photon polarization qubit have been characterized, one could appropriately engineer the fiber by applying a stress pattern on the fiber implementing a periodical decoupling sequence on the polarization qubit. In order to do that we shall first provide a proof-of-principle demonstration of the efficiency of bang-bang decoupling by modeling the propagation along a fiber as a sequence of birefringent crystals, placed inside an optical ring cavity. Due to birefringence, the polarization and the frequency degree of freedom of a single photon are coupled and the latter degree of freedom induces phase decoherence once is traced over. This scheme has been considered and experimentally discussed in [20], where the simplest case of multiple passes through a single birefringent crystal has been considered. Here the sequence of differently oriented crystals will provide a more general and complete model of the decoherence affecting the polarization qubit. The sequence of bang-bang operations will be realized by inserting appropriate waveplates between the crystals and we shall see that, by decreasing the length of the crystals the fidelity of the transmitted qubit increases, approaching unity when the length scale of birefringent effects, which is proportional to

the length of the crystal, becomes smaller. Here we shall focus on the simple case in which the birefringent crystals are identically oriented. This case reproduces all the features of polarization maintaining (PM) fibers, which are characterized by a *fixed* orientation of the fast and slow axes. In these fibers PMD is enhanced through an asymmetric cladding, and polarization decoherence is dramatically present. We show here that bang-bang decoupling can significantly suppress decoherence already in this case and preserve the photon polarization for a very large number of passes through the ring cavity, which means very long propagation distances along a PM fiber.

II. THE PROPOSED EXPERIMENT

The aim of our work is the experimental realization of an active fast manipulation of photon polarization states devoted to the reduction of polarization decoherence which is due to the coupling with the frequency degree of freedom. As a first test we consider a table-top realization based on a ring cavity configuration, for which we derive some analytical results which will be then verified by numerical simulations. The ring cavity scheme is depicted in Fig. 1. A pulsed diode laser (LD) with wavelength $\lambda_0 = 806$ nm is injected in the cavity through the output mirror with a reflectivity of $\sim 95\%$, which also allows the partial retrieval of the pulses after each round trip, whose duration will be around 10 ns. The cavity has been designed such that it is possible to insert in one arm a number of birefringent crystals (BCs), which simulate decoherence in a controlled way, and an opportune sequence of wave plates representing the unitary operations of the bang-bang control. We have already implemented a polarization entangled photon source to directly test the setup at the single photon level [21].
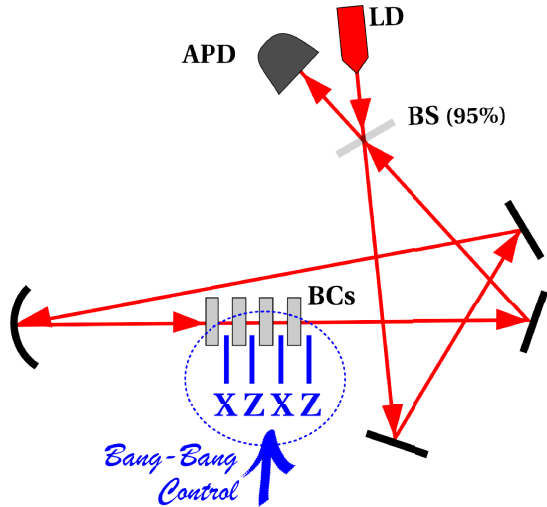
Fig. 1. Schematics of the cavity for the storage and manipulation of photons. The decoherence induced in one arm either by birefringent crystals or PM optical fiber (BCs), is expected to be recovered by the use of the Bang-Bang Control through the unitary operations $\mathbb{X}\mathbb{Z}\mathbb{X}\mathbb{Z}$. LD is a diode laser; APD is a avalanche-photodiode; BS is a beam-splitter with 95% reflectivity.

III. THE MODEL

Let's consider a birefringent crystal of length L with *fast* and *slow* index of refraction n_f and n_s, respectively. Polarization input state parallel to the slow (fast) axis acquires a phase $\phi_s = \omega n_s L/c$ ($\phi_f = \omega n_f L/c$). The action of the birefringent crystal on a polarization input state in the frame parallel to the crystal axes is given by the unitary operator

$$\mathbb{P}(\phi) \doteq \left[\begin{array}{cc} \mathrm{e}^{\mathrm{i}\phi_s} & 0 \\ 0 & \mathrm{e}^{\mathrm{i}\phi_f} \end{array} \right] = \mathrm{e}^{\mathrm{i}\Phi} \mathrm{e}^{-\mathrm{i}\frac{\phi}{2}\sigma_Z}, \quad (1)$$

with $\phi = \phi_f - \phi_s$ and $\Phi = (\phi_f + \phi_s)/2$. In a reference frame in which the crystal axes are rotated at an angle θ, the transformation of eq. (1) generalizes to

$$\mathbb{U}(\theta, \phi) = \mathbb{R}(\theta)\mathbb{P}(\phi)\mathbb{R}^\dagger(\theta), \quad (2)$$

with

$$\mathbb{R}(\theta) \doteq \left[\begin{array}{cc} \cos\theta & -\sin\theta \\ \sin\theta & \cos\theta \end{array} \right] = \mathrm{e}^{-\mathrm{i}\theta\sigma_Y}. \quad (3)$$

The unitary operator in eq. (2) can be written in terms of the 2x2 Pauli matrices $\boldsymbol{\sigma} = (\sigma_X, \sigma_Y, \sigma_Z)$ as

$$\mathbb{U}(\theta, \phi) \doteq \mathrm{e}^{\mathrm{i}\Phi}\mathrm{e}^{\mathrm{i}\frac{\phi}{2}\mathbf{s_o}\cdot\boldsymbol{\sigma}}, \quad (4)$$

i.e., a rotation of an angle ϕ around the axes defined by the vector

$$\mathbf{s_o} = [-\sin(2\theta), 0, \cos(2\theta)]. \quad (5)$$

A. Without bang-bang control

During the propagation through a sequence of $4n$ crystals, with different lengths and different orientations of the axes, an input polarization state is transformed by the unitary operator

$$\mathbb{U}_{4n} = \prod_{j=1}^{4n} \mathbb{U}(\theta_j, \phi_j), \quad (6)$$

which represents a model for a generic single mode (SM) optical-fiber. On the contrary, all axes aligned along the same direction, forming an angle θ with the reference frame, can be considered as a model for a PM optical-fiber.

We focus on the analysis of the latter with a fixed crystal length. In this case ϕ is the same for each crystal but depends on the frequency; therefore

$$\mathbb{U}_{4n}(\theta, \phi) = [\mathbb{U}(\theta, \phi)]^{4n} = \mathbb{U}(\theta, 4n\phi) \quad (7)$$
$$= \mathbb{R}(\theta)\mathbb{P}(4n\phi)\mathbb{R}^\dagger(\theta),$$

where n is the number of cavity round-trips. We consider an electromagnetic input field with an amplitude spectrum $\mathcal{A}(\omega)$, normalized such that $\int d\omega |\mathcal{A}(\omega)|^2 = 1$, and a frequency independent polarization state $|p\rangle_{in}$. The total input state of the input field is therefore

$$|\psi\rangle_{in} = \int d\omega \mathcal{A}(\omega) |\omega\rangle \otimes |p\rangle_{in}. \quad (8)$$

The output polarization state is given by the reduced density matrix obtained by tracing out the frequency degree of freedom

$$\hat{\rho}_{out}^{NoBB} = \int d\omega |\mathcal{A}(\omega)|^2 \, \mathbb{U}_{4n}(\theta, \phi)\hat{\rho}_{in}\mathbb{U}_{4n}^\dagger(\theta, \phi), \quad (9)$$

with

$$\hat{\rho}_{in} = |p\rangle\langle p| = \frac{1}{2}\left[\mathbb{I} + \mathbf{p}_{in}\cdot\boldsymbol{\sigma}\right], \qquad (10)$$

where $\mathbf{p}_{in}$ is the Stokes (or equivalently, Bloch) vector of the input polarization state. Note that the unitary operator $\mathbb{U}_{4n}(\theta,\phi)$ depends on the frequency through the parameter $\phi = \phi(\omega) = \omega\Delta n L/c$, with $\Delta n = n_f - n_s$, and the reduced density matrix can be derived as an average over the frequency spectrum, $\mathcal{A}(\omega)$ [20]

$$\hat{\rho}_{out}^{NoBB} = \frac{1}{2}\left[\mathbb{I} + \mathbf{p}_{out}^{NoBB}\cdot\boldsymbol{\sigma}\right] \qquad (11)$$

The output Stokes vector $\mathbf{p}_{out}^{NoBB}$ is related to the input one, $\mathbf{p}_{in}$, by the averaged Muller matrix, $\langle\hat{\mathbf{V}}^{NoBB}[\theta,\phi(\omega)]\rangle$, through the expression

$$\begin{aligned}\mathbf{p}_{out}^{NoBB} &= \langle\hat{\mathbf{V}}^{NoBB}[\theta,\phi(\omega)]\rangle\,\mathbf{p}_{in}\\ &= \int d\omega|\mathcal{A}(\omega)|^2\,\hat{\mathbf{V}}^{NoBB}[\theta,\phi(\omega)]\,\mathbf{p}_{in}.\end{aligned} \quad (12)$$

The polarization output state is in general a mixed state, whose purity depends on the crystal parameters, as well on the polarization input state. Only for a monochromatic input, i.e., an infinitely narrow pulse spectrum, the state remains pure. An explicit expression for the Muller matrix in terms of the angle $4n\phi$ and the vector $\mathbf{s_0}$ given in eq. (5) can be found according to the relation $\mathbf{V}\boldsymbol{\sigma} = \mathbb{U}^\dagger\boldsymbol{\sigma}\mathbb{U}$:

$$\hat{\mathbf{V}}^{NoBB}(\theta,\phi) = \mathbf{R}_Y(2\theta)\mathbf{R}_Z(4n\phi)\mathbf{R}_Y^\dagger(2\theta), \qquad (13)$$

where $\mathbf{R}_k(\alpha)$ represents an O(3) rotation of an angle α along the k-axis.

B. With bang-bang control

To overcome the reduction of purity of the state due to the crystals birefringence and the nonzero bandwidth of the photon pulse we consider now a bang-bang control. This control is realized including opportune rotations between the crystals (see Fig. 1). It has been shown [3], [19] that a bang-bang control on the polarization of the field can be realized by the two non-commuting rotations $\mathbb{Z} \doteq \sigma_Z$ and $\mathbb{X} \doteq \sigma_X$ between adjacent crystals. The evolution of the polarization state after n cavity round trips in the presence of the bang-bang control is therefore

$$\mathbb{U}_{BB}(\theta,\phi) = [\mathbb{Z}\mathbb{U}(\theta,\phi)\mathbb{X}\mathbb{U}(\theta,\phi)]^{2n}. \qquad (14)$$

This control sequence cancels decoherence at first order in $\phi \sim \Delta n L$, but it is possible to devise more involved control sequences able to cancel decoherence at higher orders [3]. Using eq. (14), it is possible to write for the reduced density matrix of the output polarization an expression analogous to that of eq. (11)

$$\hat{\rho}_{out}^{BB} = \frac{1}{2}\left[\mathbb{I} + \mathbf{p}_{out}^{BB}\cdot\boldsymbol{\sigma}\right], \qquad (15)$$

with

$$\mathbf{p}_{out}^{BB} = \langle\hat{\mathbf{V}}^{BB}[\theta,\phi(\omega)]\rangle\,\mathbf{p_{in}}, \qquad (16)$$

and $\langle\hat{\mathbf{V}}^{BB}[\theta,\phi(\omega)]\rangle$ the average Muller matrix in the presence of bang-bang. In fact it is possible to derive the expression

$$[\mathbb{Z}\mathbb{U}(\theta,\phi)\mathbb{X}\mathbb{U}(\theta,\phi)]^2 = e^{4i\Phi}e^{i\alpha(\theta,\phi)\mathbf{s}(\theta,\phi)\cdot\boldsymbol{\sigma}}, \quad (17)$$

with the angle $\alpha(\theta,\phi)$ satisfying the relation

$$\sin\left[\frac{\alpha(\theta,\phi)}{2}\right] = \sin^2\left(\frac{\phi}{2}\right)\sin(4\theta), \qquad (18)$$

and the 3D vector $\mathbf{s}(\theta,\phi)$ given by

$$\mathbf{s}(\theta,\phi) = \begin{bmatrix} 0 \\ \dfrac{\cos^2(\phi/2)+\cos(4\theta)\sin^2(\phi/2)}{\sqrt{1-[\sin^2(\phi/2)\sin(4\theta)]^2}} \\ -\dfrac{\sin\phi\sin(2\theta)}{\sqrt{1-[\sin^2(\phi/2)\sin(4\theta)]^2}} \end{bmatrix}. \quad (19)$$

The Muller matrix in the bang-bang case $\hat{\mathbf{V}}^{BB}[\theta,\phi]$ assumes a form similar to that without bang-bang of eq. (13), that is,

$$\hat{\mathbf{V}}^{BB}(\theta,\phi) = \mathbf{R}_X(2\theta_{BB})\mathbf{R}_Z\left[2n\alpha(\theta,\phi)\right]\mathbf{R}_X^\dagger(2\theta_{BB}), \tag{20}$$

where the angle θ_{BB} is defined by the relation

$$\tan(2\theta_{BB}) = \frac{\cos^2(\phi/2) + \cos(4\theta)\sin^2(\phi/2)}{\sin\phi\sin(2\theta)}. \qquad (21)$$

A first important consequence of these results is that the bang-bang control allows a *complete elimination of decoherence, at all orders, for any input polarization state* when the crystal orientation θ is equal to $0°$ and $45°$, i.e., whenever the birefringent crystal axes are parallel to one of the two control operations σ_X or σ_Z. In fact, eq. (18) shows that when $\sin(4\theta) = 0$, that is, $\theta = 0°, 45°$, it is $\alpha(\theta,\phi) = 0$, implying that the Muller matrix becomes equal the 3×3 identity matrix. This is a first significant benefit of the bang-bang control which also suggests that decoherence suppression will be relevant also at orientations θ not too far from $0°$ and $45°$.

C. Gaussian field spectrum

We consider now a Gaussian spectrum for the input field given by

$$\mathcal{A}(\omega) = (\pi\sigma_\omega^2)^{-1/4}\exp\left\{-\frac{(\omega-\omega_0)^2}{2\sigma_\omega^2}\right\}, \qquad (22)$$

were $\sigma_\omega = 2\pi c\Delta\lambda/\lambda_0^2$, with $\lambda_0 = 2\pi c/\omega_0$, and $\Delta\lambda$ represents the bandwidth of the spectrum in wavelength. The average over the frequency becomes an integral over a Gaussian measure with standard deviation σ_ω. As the frequency dependence of the integrand comes out only through the phase $\phi(\omega)$, and assuming a slow variation of the index of refraction with respect to the frequency, the integrals can be transformed as an average over a Gaussian measure, $d\mu_\phi$, centered in $\phi_0 = 2\pi\Delta n L/\lambda_0$ with standard deviation $\sigma_\phi = \Delta n L\sigma_\omega/c = 2\pi\Delta n L\Delta\lambda/\lambda_0^2$

$$d\mu_\phi = \frac{d\phi}{\sqrt{\pi\sigma_\phi^2}}e^{-\frac{(\phi-\phi_0)^2}{\sigma_\phi^2}} \qquad (23)$$

In order to have a simple and effective characterization of the performance of the bang-bang control, we quantify the degradation of the polarization state due to decoherence in terms of two quantities, the *average purity* $\langle \text{Tr}[\hat{\rho}_{out}^2] \rangle$, and the *effective average fidelity* $\langle \text{Tr}[\hat{\rho}_{out}\hat{\rho}_{out}^0] \rangle$. Both quantities are independent of the input polarization because they are averaged over a uniform distribution over the Bloch sphere of pure input polarization states. In particular, the effective average fidelity gives the probability of recovering at the output the ideal polarization state one would have in the absence of PMD, i.e., the state $\hat{\rho}_{out}^0$ obtained in the case of a monochromatic field at frequency ω_0. It is possible to derive the exact analytical expression for both quantities for the case without bang-bang control. Using eq. (13) and performing the averages over frequency and over the Bloch sphere, we get

$$\langle \text{Tr}[\hat{\rho}_{out}^2] \rangle^{NoBB} = \frac{2}{3} + \frac{1}{3} \exp[-8n^2\sigma_\phi^2], \quad (24)$$

$$\langle \text{Tr}[\hat{\rho}_{out}\hat{\rho}_{out}^0] \rangle^{NoBB} = \frac{2}{3} + \frac{1}{3} \exp[-4n^2\sigma_\phi^2]. \quad (25)$$

Both quantities show a Gaussian decay as a function of the number of n and do not depend on the orientation θ and the mean phase $\phi_0 = \omega_0 \Delta n L/c$, but only on the phase variance σ_ϕ^2. The asymptotic limit $n \to \infty$ of $2/3$ corresponds to the situation where the averaged Muller matrix $\langle \hat{\mathbf{V}}^{NoBB}(\theta, \phi) \rangle$ is the projector over the direction determined by the Stokes vector $\mathbf{s_0}$ of eq. (5). This means that the two polarization states with Stokes vector $\pm\mathbf{s_0}$ are unaffected by the propagation through the crystals, while all polarization states with Stokes vector orthogonal to $\mathbf{s_0}$ are transformed into the maximally mixed state $\hat{\rho}_{out}^{NoBB} = \mathbb{I}/2$ for large n. The polarization states unaffected by the propagation represent the so-called *principal states of polarization* (PSPs) of the optical system, and they corresponds to the linear polarization states at θ and $\theta+\pi/2$. Their existence is evident already from eq. (4), implying that the states with Stokes vector $\pm\mathbf{s_0}$ are unaffected by the crystal.

In the case of the bang-bang control, the average over the Gaussian spectrum is less simple because of the involved expressions of $\alpha(\theta, \phi)$ and $\mathbf{s}(\theta, \phi)$, and therefore analytical results are more difficult to derive. *We expect however to find the same asymptotic limit of $2/3$ for both the average purity and effective fidelity for $n \to \infty$ because also in the presence of bang-bang appropriate PSPs exist*, and the asymptotic averaged Muller matrix $\langle \hat{\mathbf{V}}^{BB}(\theta, \phi) \rangle$ is the projector over the corresponding Stokes direction. It is possible to see that the PSPs in the presence of bang-bang are the polarization states with Stokes vector $\pm\mathbf{s}(\theta, \phi_0)$, i.e., that given by eq. (19) with $\phi = \phi_0 = 2\pi\Delta n L/\lambda_0$. This can be proved by showing that if the state with Stokes vector $\mathbf{s}(\theta, \phi_0)$ is taken as input state, the same state is recovered in the limit $n \to \infty$. In fact, using eqs. (15), (17) and (23), one can write for the Stokes vector after n cavity round trips, $\mathbf{p}_{out,n}^{BB}$,

$$\mathbf{p}_{out,n}^{BB} \cdot \boldsymbol{\sigma} = \int d\mu_\phi e^{in\alpha(\theta,\phi)\mathbf{s}(\theta,\phi)\cdot\boldsymbol{\sigma}} [\mathbf{p}_{in} \cdot \boldsymbol{\sigma}] e^{-in\alpha(\theta,\phi)\mathbf{s}(\theta,\phi)\cdot\boldsymbol{\sigma}}$$

$$= \int d\mu_\phi \{\cos[2n\alpha(\theta,\phi)] \mathbf{p}_{in} \cdot \boldsymbol{\sigma}+$$
$$+ \sin[2n\alpha(\theta,\phi)] [\mathbf{p}_{in} \times \mathbf{s}(\theta,\phi)] \cdot \boldsymbol{\sigma} +$$
$$+ [1 - \cos[2n\alpha(\theta,\phi)]] [\mathbf{p}_{in} \cdot \mathbf{s}(\theta,\phi)] [\mathbf{s}(\theta,\phi) \cdot \boldsymbol{\sigma}]\}. \quad (26)$$

It is possible to see that the average of the sinusoidal terms tends to zero in the limit $n \to \infty$ so that

$$\mathbf{p}_{out,\infty}^{BB} \cdot \boldsymbol{\sigma} = \int d\mu_\phi [\mathbf{p}_{in} \cdot \mathbf{s}(\theta,\phi)] [\mathbf{s}(\theta,\phi) \cdot \boldsymbol{\sigma}]. \quad (27)$$

If we now choose $\mathbf{p}_{in} = \mathbf{s}(\theta, \phi_0)$ and rewrite $\mathbf{s}(\theta, \phi) = \mathbf{s}(\theta, \phi_0) + \boldsymbol{\Delta}\mathbf{s}(\theta, \phi)$ in eq. (27), and use the fact that $\mathbf{p}_{in} = \mathbf{s}(\theta, \phi_0)$ is of unit norm, we get

$$\mathbf{p}_{out,\infty}^{BB} \cdot \boldsymbol{\sigma} = \int d\mu_\phi [1 + \mathbf{s}(\theta,\phi_0) \cdot \boldsymbol{\Delta}\mathbf{s}(\theta,\phi)]$$
$$\times [\mathbf{s}(\theta,\phi_0) \cdot \boldsymbol{\sigma} + \boldsymbol{\Delta}\mathbf{s}(\theta,\phi) \cdot \boldsymbol{\sigma}]. \quad (28)$$

It is then possible to see that the average over the Gaussian measure of eq. (23) of all the terms containing $\boldsymbol{\Delta}\mathbf{s}(\theta, \phi)$ is zero, so that we arrive at

$$\mathbf{p}_{out,\infty}^{BB} \cdot \boldsymbol{\sigma} = \mathbf{s}(\theta, \phi_0) \cdot \boldsymbol{\sigma}, \quad (29)$$

that is, the state with Stokes vector $\mathbf{s}(\theta, \phi_0)$ is a PSP of the optical system with the bang-bang controls.

This means that in the asymptotic limit of a very large number of cavity round trips (i.e., for very long fibers), bang-bang control does not improve the purity and the fidelity of the transmitted polarization state. Nonetheless, bang-bang control is still very effective in suppressing the decoherence due to PMD, because, as it will be shown by the numerical results of the next section, the decay to the asymptotic limit of $2/3$ of the average purity and fidelity for large n is progressively slower for decreasing crystal lengths, that is, for closer controlled rotations.

IV. NUMERICAL SIMULATIONS

Monte Carlo simulations to find results for the bang-bang control on the polarization have been performed. Firstly we have tested the simulation recovering the analytical results for the case without bang-bang control. The average purity $\langle \text{Tr}[\hat{\rho}_{out}^2] \rangle$ and the effective average fidelity $\langle \text{Tr}[\hat{\rho}_{out}\hat{\rho}_{out}^0] \rangle$ are reported in Fig. 2 as a function of the number of passages n through the set of 4-crystals, set to an angle $\theta = 22.5°$ with respect to the σ_Z reference frame, for three different values of the crystal length $L = 0.75/x$ mm, with $x = 32, 64$ and 128. As expected, for the longer crystal $L = 0.75/32$ mm (dotted-line in Fig. 2), decoherence effects are larger. For each n, the average over the input states and over the frequency has been performed by considering the evolution of 96 pure states, randomly chosen according to a uniform distribution over the Bloch sphere, and with 100 values of the frequency, generated according to a Gaussian distribution with central wavelength $\lambda_0 = 806$ nm and bandwidth $\Delta\lambda = 10$ nm. The numerical simulations reproduce the analytical results given by eqs. (24) and (25), with the expected asymptotic limit of $2/3$.
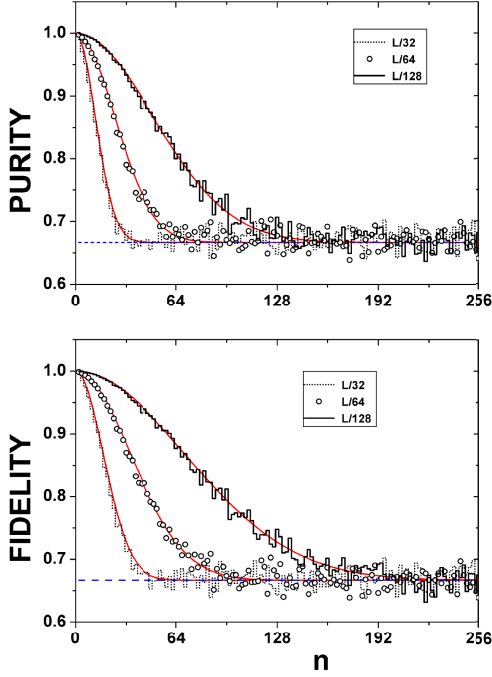
Fig. 2. *Average purity* and *effective average fidelity* as function of the passages, n, in the set of 4-crystals without bang-bang control. The crystal length is $L = 0.75/x$ mm, with $x = 32, 64$ and 128 for the black-dotted lines, circle symbols and black-solid line, respectively. For each n the two quantities are evaluated as average over 96 polarization pure states uniformly distributed over the Bloch sphere, and 100 values of the frequency generated according to a Gaussian distribution with central wavelength $\lambda_0 = 806$ nm, and bandwidth $\Delta\lambda = 10$ nm. The difference between the index refraction for the fast and slow axes is fixed to $\Delta n = 0.009$, and the axes orientation to $\theta = 22.5°$. The red lines are the curves plotted according to eqs. (24) and (25), without fitting-parameters.

Fig. 3. Average purity and effective average fidelity as function of the passages, n, in the set of 4-crystals oriented at $\theta = 22.5°$. The plots with black-lines correspond to the case of the propagation through the crystal without bang-bang control, instead with red-lines we report the plots corresponding to the propagation through the crystals with bang-bang control. The blue-dashed line correspond to the asymptotic limit for both the quantities: $2/3$. For each n the purity and fidelity are evaluated as average over 96 polarization pure states uniformly distributed over the Bloch sphere, and 100 values of the frequency generated according to a Gaussian distribution with the same parameters and crystal lengths used for the plots in Fig. 2.

We have then performed a comparison of the previous results without control with those in the presence of the bang-bang control. For each number of passages n through the set of 4-crystals (plus the operations for the bang-bang control), set again at $\theta = 22.5°$, we have performed the average over the Bloch sphere and the frequency in the same way as in the no-bang-bang case.

The average purity and the effective average fidelity are reported in Fig. 3, as a function of n, again for the previous three different values of the crystal length. As expected, for the longer crystal, $L = 0.75/32$ mm (dotted-lines in the purity plots of Fig. 3), the effect of the bang-bang control is not optimal and the purity and the fidelity are higher than those with no bang-bang control only up to ~ 48 passages. The expected asymptotic value $2/3$ is recovered for both quantities and is quickly reached for the longer crystals. Instead for the smaller crystal length, $L = 0.375/128$ mm (solid-lines in Fig. 3), the bang-bang control becomes much more efficient and keeps the purity and the fidelity up to values higher than 0.95 for almost 128 passages.

In Fig. 4 are reported the average purity and effective average fidelity as function of the angle θ. The average has been taken over 192 polarization pure states uniformly distributed over the Bloch sphere, and 100 values of the frequency generated according to the Gaussian distribution with the same parameters used for the plots of Fig. 3. The crystal length has been fixed to $L = 0.375/32$ mm, and the number of passages to $n = 64$. For the case without bang-bang control (black-dotted line), the values of the two average quantities does not depend on the angle θ as expected, and the asymptotic limit is 2/3 (blue-dashed line).

Instead, the results in the presence of the bang-bang control are significantly better for a large interval of values of the crystal orientation θ. This is a consequence of the complete elimination of decoherence, at all orders, for any input polarization state when $\theta = 0°, 45°$ discussed in the previous section and which is clearly visible in Fig. 4.

Finally, another important parameter to be considered is the frequency bandwidth of the field. In Fig. 5 the results for the average purity and effective average fidelity as function of the bandwidth for $\Delta\lambda = 1, 5, 10$ nm are reported for a crystal length $L = 0.75/32$ mm. As expected, a narrower bandwidth allows more passages before the purity and fidelity decrease to the common asymptotic limit of $2/3$, but it does not improve the factors of merit associated to the bang-bang control with respect to the one without control.
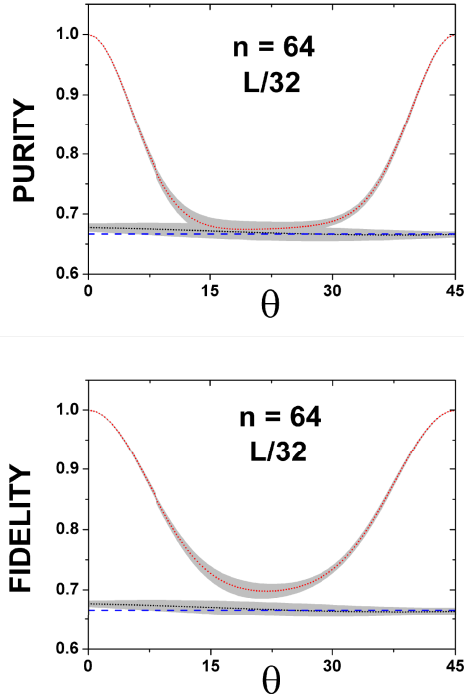
Fig. 4. Average purity and effective average fidelity as function of the angle θ for a crystal length $L = 0.375/32$ mm, and $n = 64$, corresponding to the vertical dotted lines in Fig. 3. The plots with dotted-black lines correspond to the case without bang-bang control, instead with dotted-red lines are reported the plots with bang-bang control, and the blue-dashed lines the asymptotic limit $2/3$. For each θ the quantities have been evaluated over 192 polarization pure states, and 100 values of the frequency as described in Fig. 3. The dotted line represent the average of those evaluation over 4-trials, and the gray-areas indicates the standard deviation with respect to these trials.

V. CONCLUSION

We have proposed a proof-of-principle demonstration of the potentialities of bang-bang techniques for suppressing the decoherence on the polarization of photon pulses along optical fibers. In addition to the important application for long distance, high speed telecommunication in optical fibers, this method may find applications in other systems in which one wants to reduce unwanted birefringence. Finally, on the conceptual side, our work provides a simple system in which to test the ideas of bang-bang control.

REFERENCES

[1] U. Haeberlen, High Resolution NMR in Solids: Selective Averaging (Academic Press, New York, 1976).
[2] M. A. Nielsen, and I. L. Chuang, Quantum Computation and Quantum Information (Cambridge University Press, Cambridge, UK, 2000).
[3] L. Viola, E. Knill, and S. Lloyd, Phys. Rev. Lett. **82**, 2417 (1999).
[4] M. S. Byrd and D. A. Lidar, Phys. Rev. Lett. **89**, 047901 (2002); E. M. Fortunato et al., New J. Phys. **4**, 5.1 (2002).
[5] N. Boulant et al., Quantum. Inf. Proc. **1**, 135 (2002); K. Khodjasteh and D. A. Lidar, Phys. Rev. A **68**, 022322 (2003).
[6] D. Vitali and P. Tombesi, Phys. Rev. A **59**, 4178 (1999); *ibid.* **65**, 012305 (2002).
[7] See e.g. L. Viola, Phys. Rev. A **66**, 012307 (2002).
[8] L.-A. Wu and D.A. Lidar, Phys. Rev. A **70** 062310 (2004).
[9] N. Gisin et al., Rev. Mod. Phys. **74**, 145 (2002).
[10] C. D. Poole, Opt. Lett. **13**, 687 (1988).
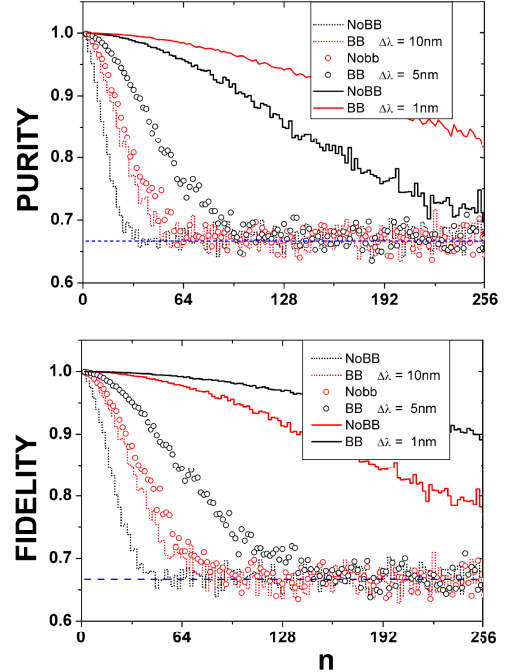
Fig. 5. For each n the average purity and effective average fidelity are evaluated as average over 96 polarization pure states uniformly distributed over the Bloch sphere, and 100 values of the frequency generated according to a Gaussian distribution with central wavelength $\lambda_0 = 806$ nm, and bandwidth $\Delta\lambda = 1, 5, 10$ nm, reported as solid lines, circle symbols and dotted-lines, respectively. The red-lines correspond to the bang-bang control, instead black-lines without control. The crystals length is fixed to $L = 0.75/32$ mm, and the other parameters are the same as in Fig. 3.

[11] C. D. Poole, Opt. Lett. **14**, 523 (1989).
[12] C. D. Poole, J. H. Winters, and J. A. Nagel, Opt. Lett. **16**,372 (1991).
[13] N. Gisin, J.P. Von Der Weid, and J.P. Pellaux, IEEE J. Lightwave Technology, **9**, 821-827 (1991).
[14] N. Gisin, and J.P. Pellaux, Optics Commun., **89**, 316-323 (1992).
[15] D. A. Nolan, X. Chen, M.-J. Li, IEEE J. Lightwave Technology,**22**, 1066 (2004).
[16] A. Galtarossa, C. R. Menyuk (Editors), *Polarization Mode Dispersion*, Springer (2005).
[17] A. J. Barlow, J. J. Ramskov-Hansen, and D. N. Payne, Applied Optics, **20** 2962 (1981).
[18] A. C. Hart Jr., R. G. Huff, K. L. Walker, US patent 5 298 047, Mar. 29 1994.
[19] S. Massar, and S. Popescu, arXiv:physics/0606028.
[20] A. J. Berglund, arXiv:physics/0010001.
[21] A. Ceré, M. Lucamarini, G. Di Giuseppe, and P. Tombesi, Phys. Rev. Lett. **96**, 200501 (2006).